

Extended Magic-Angle Spinning

A. Samoson

Volume 9, pp 59–64

in

Encyclopedia of Nuclear Magnetic Resonance

Volume 9: Advances in NMR

(ISBN 0471 49082 2)

Edited by

David M. Grant and Robin K. Harris

© John Wiley & Sons, Ltd, Chichester, 2002

Extended Magic-Angle Spinning

A. Samoson

National Institute of Chemical Physics and Biophysics, Tallinn, Estonia

1	Introduction	1
2	Principles of High Speed Rotation	1
3	Practical Considerations	2
4	Applications Specific to High Speeds	3
5	Conclusions	5
6	References	5

1 INTRODUCTION

Fast mechanical rotation is used in diverse situations, ranging from the gentle breeze of a dental drill, spinning at 5–7 kHz, to the roar of aircraft jet turbines with 500 m s^{-1} tip speeds. Rotation frequencies of 23 kHz have been achieved with microfabricated single crystal silicon turbines, representing a level of fast developing microelectromechanical systems.¹ The ultimate example was recently demonstrated by rotating a single molecule:² Cl_2 was polarized by a strong electrical field, oscillating at a frequency of 370 THz. Despite rapid alternation of the electric field polarity, the molecule lines up with the axis of the field. The alignment energy of 50 meV is actually about one million times larger than the proton Zeeman energy in a 11.7 T magnet. The axis of the oscillation of the electric field was then made to rotate by combining frequency modulated circularly polarized laser beams. The molecule followed adiabatically up to 4.1 THz, at this point two atoms dissociated.

Several branches of spectroscopy benefit from fast rotation. A high peripheral speed can be used to provoke Doppler shifts in gamma spectroscopy.³ Line narrowing due to a wavefunction phase summation at three different sample positions was demonstrated in ESR.⁴ However, due to exceptionally low transition energies and long relaxation rates, the most beneficial application of the fast rotation has been in NMR.

The magnetic field, used in NMR as a generator of the spin energy levels, has one inherent drawback: the axial nature. If nonoriented solid samples are studied, the observable signal sums up from all spectral transition frequencies determined by the orientation of the field direction in atomic coordinates, instead of a single scalar value required for the best resolution. The field orientation dependency can be suppressed by fast mechanical reorientation of the sample. One particular field trajectory has proven specially efficient. It is described by a rotation at an angle, derived from a root of a second order Legendre polynomial. The rotation angle is equal to the angle between the body diagonal of the cube and one of its edges

and the trajectory of the magnetic field can be regarded as an infinite collection of three orthogonal spatial directions. The intuitive explanation of the averaging effect can thus be related to a cubic approximation of SO_3 symmetry which would perfectly annihilate the original axial nature of the magnetic field. Next (and so far only) regular distributions of field directions follow octahedral symmetry. This can be shown to remove 15 interactions including rank 29 as the highest,⁵ if the interactions are classified by symmetry properties of the Legendre polynomials. The key to a scalar measurement process is the speed of the magnetic field reorientation. If the time constant is short compared to the nuclear relaxation and dephasing processes, the scalar value emerges from the spectra. Although a rotation as slow as few hundred revolutions per second (Hertz) may show an effect on the spectra, lines may still be broadened or flanked by sidebands. Higher speeds are usually advantageous and offer more experimental flexibility.

The experimental history of high resolution NMR in solids has thus been a quest for higher spinning speeds. Principally two different rotor designs have been used. First experiments used a conical rotor design, exploiting Bernoulli forces to hold the rotor in the coil.⁶ Better stability and higher speeds have been achieved by a double gas bearing system, pioneered by the group of Lippmaa in Tallinn.⁷ The design principles are relatively well mastered by now and several implementations have claimed a rotor surface speed exceeding that of the speed of sound in air. However, practical applications are limited to sub-sonic speeds by the dependable strength of the rotor material. The presence of the magnetic field limits the choice of materials to nonconductive ceramics or polymer compounds.

2 PRINCIPLES OF HIGH SPEED ROTATION

The design and successful exploitation of MAS equipment is based on a careful consideration of the stress acting on the rotor wall. The most important equation in high-speed technology of hollow rotors was given by Chree in 1891 and it relates peripheral speed, V , with the ratio of the working strength, T , to the density of the rotor wall material ρ_r ⁸

$$V^2 = \frac{T}{\rho_r} \quad (1)$$

For the filled rotors the total force, directed towards the rotor wall, can be evaluated using an analogy with a pressurized vessel (Figure 1).

Each particle with a mass dm , rotating at an angular velocity ω at a distance r from the axis of rotation, is pulled towards the periphery with the force

$$dF = dm\omega^2 r \quad (2)$$

As seen from Figure 1, the mass of the particle with density ρ can be expressed as

$$dm = r \sin \alpha \, dr h \rho \quad (3)$$

where h is a measure of the length of the rotor. Integration over the full radius of the rotor gives

$$F = \int_0^R dF = \frac{1}{3} R^2 \omega^2 \sin \alpha h \rho \quad (4)$$

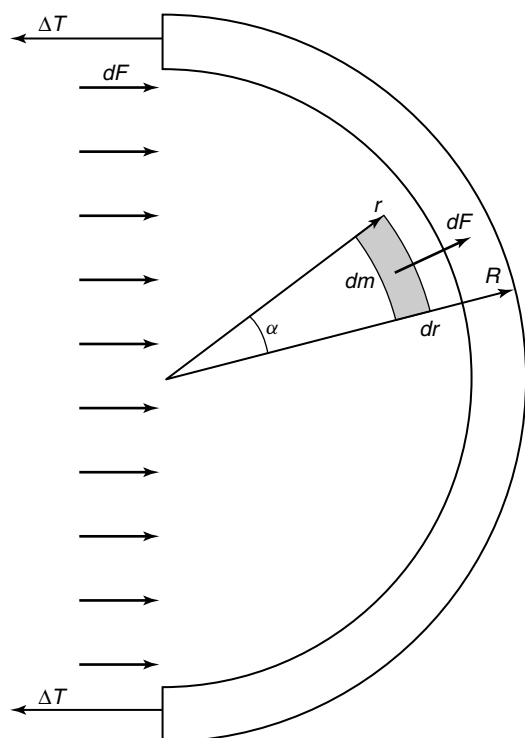


Figure 1 Evaluation of the stress force, acting on the rotor wall

The ratio of the force to surface gives a pressure on the wall of the rotor of

$$P = \frac{1}{3} R^2 \omega^2 \rho \quad (5)$$

The effective cross section, subject to a uniform pressure, can be trivially expressed as

$$S = 2Rh \quad (6)$$

The total force, acting on a semicylindrical rotor element, should be counterbalanced by a wall strength

$$PS = 2\Delta hT \quad (7)$$

where T represents the tensile strength of the material. From this the basic expression follows immediately

$$v = \frac{1}{\pi D} \sqrt{\frac{3T\Delta'}{\rho}} \quad (8)$$

where Δ' is a relative wall thickness.

Although this expression does not take into account the mass of the rotor wall, essential conclusions can be made readily. A convenient measure is a product of the rotor diameter and speed (mm \times kHz or m \times Hz). This, along with the sample density, gives the load on the rotor wall. The maximum load is determined by the wall thickness and tensile strength.

The support for high speed rotors is provided typically by gas lubricated bearings. The reason is not only the low friction, but also a certain freedom for self-balancing. This freedom is given by the gap of the order of few tens of micrometers

between the bearing surface and the rotor. The principle of self-balancing was established by De Laval in 1889. According to this principle, rotors spin about the principal axis of inertia rather than the axis of symmetry after passing critical frequencies. The critical frequencies are determined by the stiffness of the bearing and the mass of the rotor and are typically of the order of a few kilohertz for high speed rotors. A brief reduction of the bearing gas pressure lowers the stiffness and may promote passing of the resonance region during the rotor startup. Many details about construction of turbines with gas driven rotors can be found in a seminal paper by Doty and Ellis.⁹

3 PRACTICAL CONSIDERATIONS

Obviously, the most straightforward way to increase the top speed that is still sustainable by the rotor is to reduce the rotor diameter. A further improvement can be brought about by a careful selection of the rotor material, due to the inverse square root dependency on the tensile strength. For polymers, the tensile strength is determined by a limit of spatial expansion. A relatively low Young's modulus of most polymers prevent them from reaching high speeds, since rotor expansion is sufficient to quench a lubrication of the gas bearing. Better performance can be expected from more rigid ceramics, despite their brittleness. For nonductile ceramics the tensile strength is set by a fracture limit. A rigorous estimation of the critical rotation frequency, associated with material disintegration, is complicated for technical ceramic materials. An unrealistically detailed picture of microscopic processes is required. The mechanical properties of two frequently used compounds, zirconia and silicon nitride, depend sensitively on their preparation history. Both are typically powder sintered, resulting in quite inhomogeneous structure. They are characterized by an average grain size, the grain size distribution and adhesion quality. Zirconia derives its strength from a martensitic phase transformation. At a room temperature, zirconia is stable in its monoclinic crystal phase. With special processing, parts of the material can be made to retain a high-temperature tetragonal phase, which is 3–5% more compact.¹⁰ If this partially stabilized zirconia (PSZ) is subjected to a mechanical load, cracks eventually start to form. High stresses around the crack tip trigger the expansive phase transformation to low density form, squeezing further crack propagation.

Various (semi)macroscopic parameters are used to estimate the mechanical properties of the ceramic materials. The most widespread property, fracture toughness, requires a knowledge of critical flaw size and gives only an indirect estimate for the rupture limit.¹¹ More pertinent flexural strength is estimated usually from bending tests. The three point bending test characterizes a material only over a relatively small volume; four point bending data are more representative. Overall volume performance is further characterized by a Weibull modulus, m . For NMR rotors, where material strength over the entire specimen is important, $m = 30$ can be considered to provide a reasonable confidence for the strength values. Comparing data from different ceramic providers suggest that tensile strengths of 500–800 MPa can be expected for a well prepared material. This value may change with thermal chocking and continuous stress, especially for zirconia. The strength reduces also with

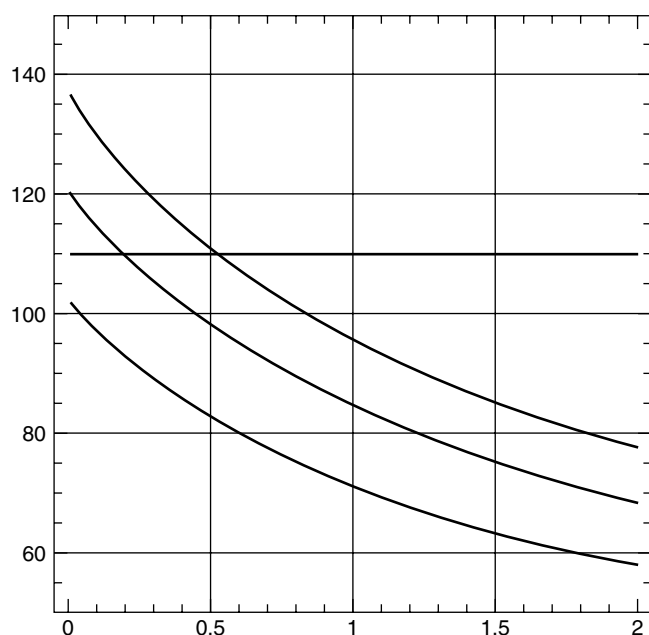


Figure 2 Dependence of the critical speed–diameter product on the ratio of sample density to rotor density. Three plots are given for different relative (i.e., divided by density) tensile strengths 900/6, 700/6 and 500/6 MPa cm³ g⁻¹, for a wall thickness $\Delta = 0.2$. Horizontal line shows the speed of sound at the rotor surface

an increase of temperature, noticeably already by a few hundred degrees. More involved calculations, which also account for the rotor wall weight, are presented graphically in Figure 2. A bold line marks the speed of sound in air at the surface of the rotor. For a reasonably broad range of sample densities, 100 mm kHz appears as a limit for high-strength materials. Indeed, practical realizations are in agreement with this estimate. In 1997, 2.5-mm rotors, specified up to 33–35 kHz, became commercially available.¹² Speeds of up to 50 kHz with rotors of about 2 mm diameter were demonstrated in 1999 in an academic laboratory (National Institute of Chemical Physics and Biophysics, Tallinn, Estonia).¹³ It is instructive to compare these values with the ultimate molecular rotor, as described in the introduction. Considering internuclear distance 0.26 nm at the breaking point, ca. 1000 mm kHz as a product of the maximum rotation speed and diameter can be evaluated. This is merely an order of magnitude more than achieved with the macroscopic MAS rotor.

Several artifacts accompany the high speed experiments. The sample is subjected to a stress gradient, ranging from 0 to about 10^6 g at the periphery. This may for example broaden lines of quadrupole nuclei due to piezoelectric effects. Another potential complication may be the sample heating. Friction with the surrounding atmosphere becomes quite noticeable at high speeds. As brought to the attention of the NMR community in Ref.¹⁴ the surface temperature heats up as a quadratic function of the speed.¹⁵ The isotropic shift of Pb in lead nitrate is a convenient thermometer for solid state NMR.¹⁶ Deduced temperatures, measured up to speeds 40 kHz,¹³ indeed follow closely the quadratic speed dependency (Figure 3). The upper data point was deliberately limited to 40 kHz in view of the exceptionally high density (4.53) of lead nitrate. Extrapolation to 50 kHz, and using a conversion factor 0.753 ppm degree⁻¹

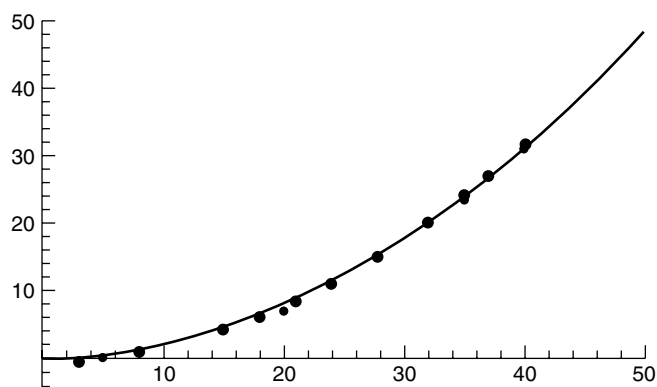


Figure 3 Dependence of ²⁰⁷Pb(NO₃)₂ temperature on the rotation speed (kHz)

predicts about a 66° increase in the rotor temperature over ambient.

The problems listed above are present for any size of rotor, reaching critical frequency of the mechanical failure. Specific for the small rotors is a loss of the signal due to a reduced amount of the sample. On the other hand, smaller resonance coils provide higher rf fields.

4 APPLICATIONS SPECIFIC TO HIGH SPEEDS

As explained above, reliable speed range can most efficiently be increased with reduction of the rotor diameter. Disregarding a trivial case of economy with expensive isotope-labelled or otherways limited samples, this is generally considered in NMR to be a disadvantage. For a majority of routine applications, spinning at 10–15 kHz gives adequate spectral quality. The problem associated with the reduction of the number of resonating nuclei is gradually alleviated by advances in magnet technology. Moreover, proliferation of the high-field magnets naturally demands faster spinning to keep in par with increased anisotropy and spectral expansion. There are also a number of special experimental situations, where the quality or even the feasibility of the measurements depend on the speed of rotation.¹⁷

Of the many nuclear recoupling methods, adiabatic two spin coherence generation, based on avoided level crossings (DREAM),¹⁸ is remarkably insensitive to specific parameters of (inter)nuclear interactions. The key mechanism of nuclear dipolar recoupling, the so-called HORROR condition,¹⁹ is only efficient when sample rotation frequency is exactly two times larger than the locking rf field amplitude. To be broadbanded enough to cover a typical carbon-13 spectrum, the rf amplitude should be comparable to (or larger than) the spectral width of carbon at the magnetic field applied. An example of the speed dependency is illustrated in Figure 4. The DREAM-filtered double quantum spectra of antamanide, cyclic decapeptide, have been recorded under otherwise identical conditions at two speeds, 20 and 40 kHz. Drastic differences can be observed in the aliphatic region of the spectra.

The rotation speed increase can be useful in the spectroscopy of quadrupole nuclei. A single quantum second-order linewidth features a definite value under the magic angle spinning conditions. For very strong quadrupole coupling constants, high speeds are required to separate the centerband

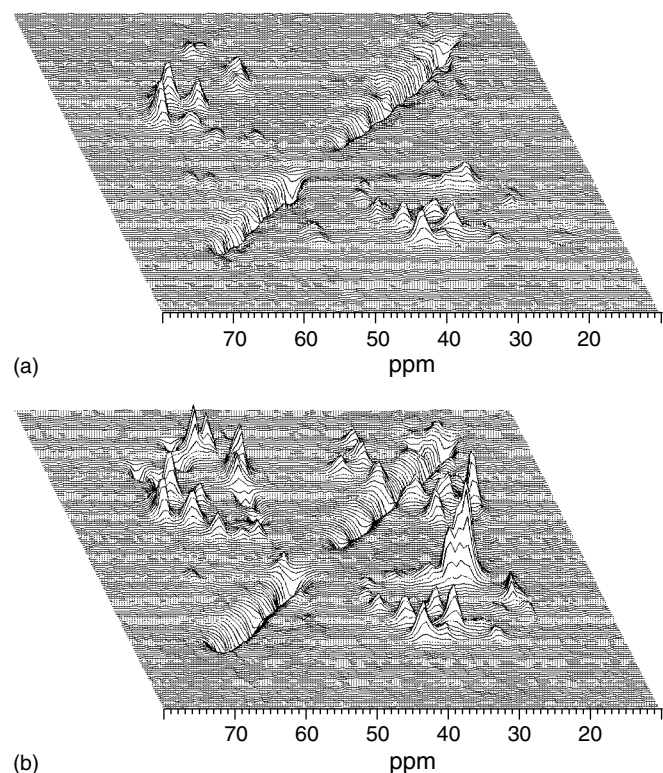


Figure 4 A comparison of 20 and 40 kHz ^{13}C DREAM spectra of antamanide. High speed spectra also exhibit some negative peaks due to the second polarization transfer during adiabatic passage. Spectra were acquired by A. Verhoeven and R. Verel, B. Meier NMR group, ETH Zürich

from sidebands.²⁰ Even more crucial is the rotation speed for registration of the satellite transitions, which are subject to a relatively strong first order quadrupole interaction.²¹ The satellite transitions have a different isotropic position, and particularly in the case of spin 5/2 are also less affected by effects of the electric field dispersion.²² This makes the satellite transition spectroscopy a valuable complementary method for high-resolution work. The gain of the satellite transition intensity as a function of the rotation speed is illustrated in Figure 5.

Perhaps the most intriguing high speed application is the possibility of suppressing homonuclear dipolar interactions. Homonuclear dipolar linebroadening in a rigid system of hydrogen atoms may exceed 50 kHz. Under magic angle spinning, the residual linewidth is only a weak function of spinning speed, decreasing linearly with first power of the speed. Multipulse sequences²³ have been developed to refocus dipolar dephasing periodically. This refocussing has been demonstrated to work also in combination with a slow sample rotation.²⁴ For rigid systems the multipulse approach can offer resolution of a few tenths of ppm. In the case of plastic crystals and the presence of fast molecular motion, the multipulse approach becomes principally less effective. It may also be technically difficult to retain stability over a sufficiently long measurement period. Figure 6 presents ^1H MAS only spectra of camphor, where J -coupling becomes visible at 50 kHz. Moving to the higher fields, fast rotation starts to provide informative spectra also for rigid systems, as shown in

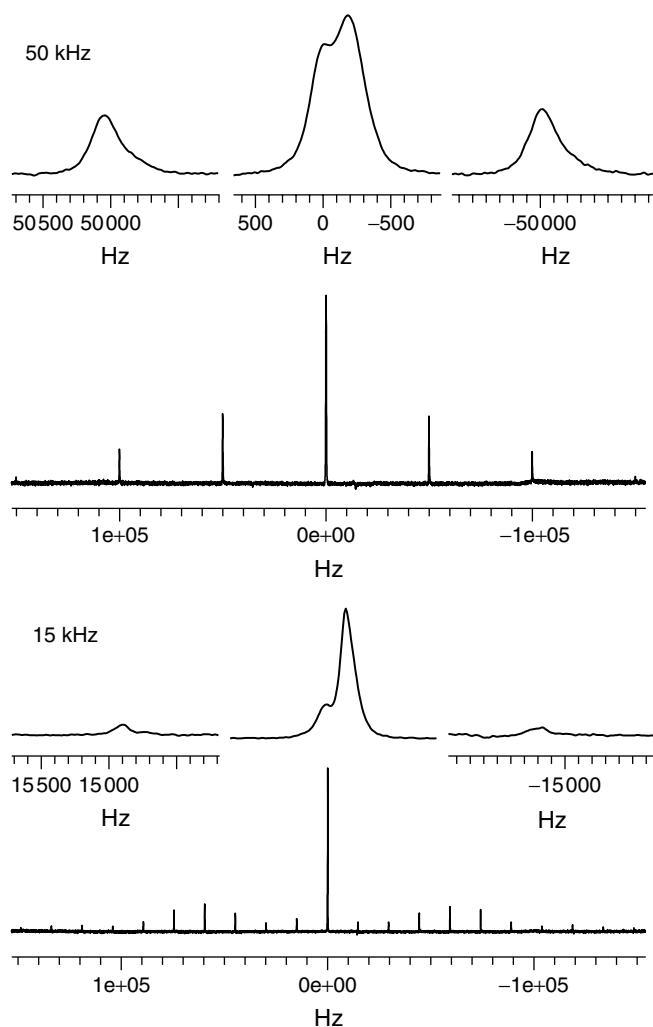


Figure 5 ^{23}Na spectra of NaNO_3 at 53 MHz. Expanded plots show centerbands and respective first sidebands, formed by the overlapping ($3/2 \rightarrow 1/2$, $-1/2 \rightarrow -3/2$) satellite transitions of the spin 3/2 nucleus. The sideband pattern in the low speed spectrum indicates a shape of the first order quadrupole broadening of the satellite transitions. At the high speed, the centerband of the satellite transition has an intensity, comparable to that of the central transition. The two peaks are shifted due to the second quadrupolar effect

Figure 7. The relative resolution grows proportionally with the field strength, since residual linebroadening retains its absolute value which depends mostly on the rotation speed. Both advantages combined bring a virtually quadratic improvement in resolution. However, a subtle deviation from this trend can already be observed in higher field spectra (831 MHz). Although the resolution is better, the absolute linewidth is clearly larger than at 500 MHz. Here a natural, susceptibility induced broadening starts to compete with the residual dipolar linewidth and no further substantial resolution enhancement is possible.²⁵ The case of high speeds as a method of improving resolution may actually turn out to be the only alternative for measurements at high fields, because several experimental parameters start to complicate the application of the multi-pulse sequences. First, it is technically more demanding to generate the required rf field strength. Secondly, the multi-pulse sequences inherently lose efficiency with

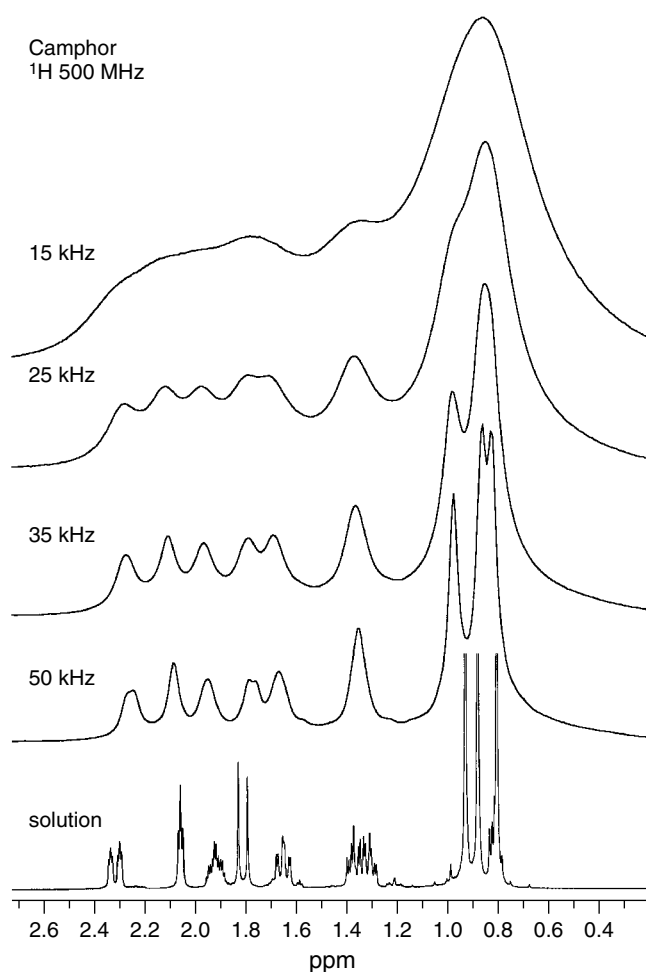


Figure 6 ^1H spectra of camphor. Lines are relatively narrow due to a molecular rotation. Nevertheless, faster rotation brings a substantial resolution enhancement, revealing finally J splitting of the two lines in the 1.8 and 2.3-ppm regions

expansion of the spectral width. This is particularly true for the spectroscopy of ^{19}F . A qualitative improvement can be observed when both high field and rotation speed are combined, as seen in Figure 8.²⁶ For several experimental situations, resolution enhancement under MAS may be not only a matter of convenience, but imperative in order to free the pulse space for specific tasks. For example in the case of inverse detection experiments, the homonuclear proton system needs to remain decoupled, while being selectively cross-polarized by nitrogen.²⁷ High rotation speeds also allow exchange of averaging order in decoupling experiments.²⁸ A very low amplitude proton rf field is then needed for well-resolved carbon spectra.

5 CONCLUSIONS

Material strength of the rotor presents a major constraint in determining the performance range of MAS. A product of rotor diameter and highest speed form a material constant, set currently to about 100 mm kH. Practical and reliable values remain about 10–20% below that, as a tribute to the statistical nature of the mechanical properties of ceramics

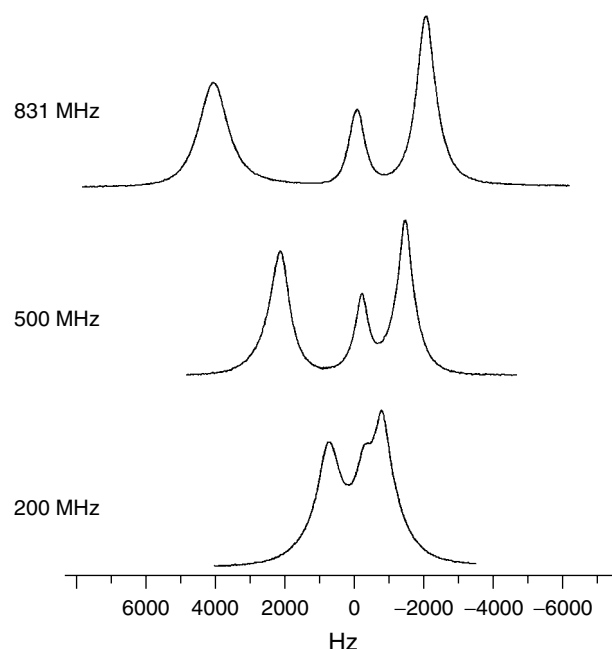


Figure 7 ^1H spectra of alanine at 200, 500 and 831 MHz. Sample rotation at 45 kHz. The 831 MHz spectrum was recorded at NRMFL

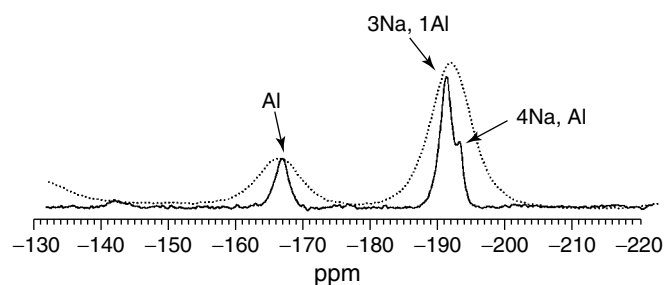


Figure 8 ^{19}F spectra of the mineral Chiolite $\text{Na}_5\text{Al}_3\text{F}_{14}$. A combined effect of the field (19.6 vs. 8.5 T) and rotation speed (40 vs. 20 kHz) confirms the existence of three different coordination environments, as indicated, with intensity ratio of 2:4:1. Spectra were recorded by L. S. Du, SUNY Stony Brook

used for the rotors. Development of the sub 2-mm rotors has allowed speeds of 50 kHz to be reached. The most immediate benefits that arise from fast MAS are likely to be found in the spectroscopy of high-gamma and quadrupole nuclei. The extended range of possible rotation frequencies provides more flexibility in choosing various matching conditions with either rf field amplitudes or spectral positions of different atomic sites. This feature may significantly facilitate atomic topology studies.

6 REFERENCES

1. L. G. Frechette, S. A. Jacobson, K. S. Breuer, F. F. Ehrlich, R. Ghodssi, R. Khanna, C. W. Wong, X. Zhang, M. A. Schmidt, and A. H. Epstein, 'Solid State Sensor and Actuator Workshop', Hilton Head Island, SC, June 4–8, 2000.
2. D. M. Villeneuve, S. A. Aseyev, P. Dietrich, M. Spanner, M. Yu. Ivanov, and P. B. Corkum, *Phys. Rev. Lett.*, 2000, **85**, 542.
3. K. Treml and H. Langho, *Z. Phys.*, 1976, **B25**, 123.

4. M. Hubrich, C. Bauer, and H. W. Spiess, *Chem. Phys. Lett.*, 1997, **273**, 259.
5. A. Samoson, B. Sun, and A. Pines, 'New Angles in Motional Averaging, Pulsed Magnetic Resonance: NMR, ESR, and Optics', Clarendon: Oxford, 1992.
6. E. R. Andrew, A. Bradbury, and R. G. Eades, *Nature*, 1958, **182**, 1659.
7. E. Lippmaa, M. Alla, A. Salumäe, and T. Tuherm, U.S. Patent 4254373, 1981.
8. C. Chree, *Proc. Cambridge Phil. Soc.*, 1981, **7**, 201.
9. F. D. Doty and P. D. Ellis, *Rev. Sci. Instrum.*, 1981, **52**, 1868.
10. R. C. Garvie, R. H. Hannink, and R. T. Pascoe, *Nature*, 1975, **258**, 703.
11. R. G. Munro and S. W. Freiman, *J. Am. Ceram. Soc.*, 1999, **82**, 2246.
12. 'Bruker Analytik GmbH', Rheinstetten-4, Germany.
13. A. Samoson and T. Tuherm, 'The Alpine Conference on Solid-State NMR', Chamonix-Mont Blanc, France, Sept. 1999, p. T3; A. Samoson, 41st ENC, Asilomar, April 2000, p. 59; A. Samoson, T. Tuherm, and J. Past, *J. Magn. Reson.*, 2001, **149**, 264.
14. T. Mildner, H. Ernst, and D. Freude, *Solid-State NMR*, 1995, **5**, 269.
15. D. Geropp, *Ing.-Arch.*, 1969, **38**, 195.
16. A. Bielecki and D. P. Burum, *J. Magn. Reson.*, 1995, **A116**, 215.
17. P. Hartmann, J. W. Zwanziger, and C. Jäger, *Solid State NMR*, 2000, **16**, 189.
18. R. Verel, M. Baldus, M. Ernst, and B. Meier, *Chem. Phys. Lett.*, 1998, **287**, 421.
19. N. Nielsen, H. Bildsoe, H. Jakobsen, and M. Levitt, *J. Chem. Phys.*, 1994, **101**, 1805.
20. A. Samoson, E. Kundla, and E. Lippmaa, *J. Magn. Reson.*, 1982, **49**, 350.
21. A. Samoson, *Chem. Phys. Lett.*, 1985, **119**, 29.
22. E. Lippmaa, A. Samoson, and M. Magi, *J. Am. Chem. Soc.*, 1986, **108**, 1730.
23. J. S. Waugh, L. Huber, and U. Haeberlen, *Phys. Rev. Lett.*, 1968, **20**, 180.
24. B. Schnabel, U. Haubenreisser, G. Scheler, and R. Müller, in 'Proceedings of the 19th Congress Ampere, Heidelberg', 1976, 441; B. C. Gerstein, R. G. Pembleton, R. C. Wilson, and L. M. Ryan, *J. Chem. Phys.*, 1977, **66**, 361.
25. A. Samoson, T. Tuherm, and Z. Gan, *Solid-State NMR*, 2001, **20**, 130.
26. L. S. Du, A. Samoson, T. Tuherm, and C. P. Grey, *Chem. Mat.*, 2000, **12**(12), 3611.
27. Y. Ishii, R. Tycko, *J. Magn. Reson.*, 2000, **142**, 199.
28. M. Ernst, A. Samoson, and B. H. Meier, *Chem. Phys. Lett.*, 2001, **348**, 293.

Acknowledgements

Material presented in this overview is partly of original nature. Underlying work was supported by the Estonian Science Foundation and several extramural grants (University of Leipzig, NHMFL in Tallahassee, ETH Zürich, SUNY Stony Brook).

Biographical Sketch

Ago Samoson, *b* 1955. Ph.D., 1984, Solid State Physics, Institute of Chemical Physics and Biophysics, and Institute of Physics, Estonia. Research associate of various degrees, National Institute of Chemical Physics and Biophysics, Tallinn, Estonia, 1978–1987, 1989–1990, 1995–; Visiting Scholar, University of California, Berkeley 1987–1989, Applications Scientist, Bruker Analytische Messtechnik, Rheinstetten, Germany, 1991–1992; Visiting Scientist, University of Uppsala, Sweden, 1993–1994. Approx. 50 publications. Current research interests: (applications of) solid state NMR, development of instrumentation.